Dielectric properties of polypyrrole doped with tosylate anion in the far infrared and microwave

G. Phillips, R. Suresh, J. Waldman, and J. Kumar
Department of Physics Engineering, University of Lowell, 1 University Avenue, Lowell, Massachusetts 01854

J. I-Chen and S. Tripathy
Department of Chemistry, University of Lowell, 1 University Avenue, Lowell, Massachusetts 01854

J. C. Huang
Department of Physics Engineering, University of Lowell, 1 University Avenue, Lowell, Massachusetts 01854

(Received 31 May 1990; accepted for publication 11 October 1990)

We report measurements of the dielectric behavior in the far infrared (10–200 cm^{-1}) and in the microwave (8.5–12.5 GHz) regime for the conducting polypyrrole (PP) doped with tosylate anion. The dielectric constants have been determined from reflection and transmission data using the Fresnel equations. The magnitude and dispersive nature of the complex index of refraction is described for a number of samples with different levels of conductivity. The ability to tailor the dielectric behavior of these materials has been demonstrated by suitably reducing the oxidized PP films. The high reflectivity in the far infrared and microwave region cannot be accounted for in terms of the Drude model defining metallic behavior. An application exploiting the large real part of the index of refraction and relatively low loss observed in the microwave region is discussed.

I. INTRODUCTION

There has been considerable effort directed towards understanding the conduction mechanisms in polymer systems since the earliest observations of metal like conductivity in *p* and *n* doped polyacetylene.[1] A great interest in electrochemically synthesized conducting polymers has been motivated by the high degree of success achieved in tailoring the mechanical, electrical, and dielectric properties of these materials. Film thickness is easily controlled when grown on an electrode by controlling the total charge. The reversibility of the doping process through oxidation and reduction and the large number of dopant ions available enable one to develop polymer systems ranging widely in conductivity from nearly perfect insulators to upper limits reaching those presently achieved in polyacetylene. The specific mechanisms responsible for conduction in these materials are a subject of intense current investigation.[2] Early spectroscopic measurements showing large metal like reflection in the far infrared (FIR) and a broad free carrier like absorption in the $\lambda = 1\,\mu$ region of the spectrum, has led some to describe these materials in terms of simple metal models.[3] Further investigations, such as the behavior of conducting polymers as a function of frequency and temperature, were inconsistent with these observations.[4] Transport property measurements also contributed to the many difficulties in characterizing the mechanisms responsible for conduction in these polymers. Positive thermopower measurements were frequently accompanied by negative and contradictory Hall effect measurement.[5] The conductivity of these materials was observed to increase with temperature as $\sigma = \sigma_0 \exp[(-T_0/T)^{1/4}]$, contrary to simple metal theory. However, this temperature dependence was consistent with hopping mechanisms associated with disordered systems and observed in amorphous semiconductors with a high intragap density of states. Additional nonmetallic behavior was evidenced by electron spin resonance (ESR) measurements[6] in which the ESR signal seemed to be independent of conductivity in heavily doped systems. ESR observations were significant in developing alternative conductive mechanisms based on bound excitations such as polarons, and bipolarons. Higher energy (1–5 eV) spectroscopic measurements have likewise been consistent with formation of localized states in the band gap.[7]

Among the many conducting polymers of current interest, polypyrrole presents many additional interesting features. Electrochemically grown conducting polypyrrole is known for its good mechanical and electrical stability. In the fully oxidized state, polypyrrole achieves conductivities in excess of $10^2\ \Omega^{-1}\ cm^{-1}$.

The dielectric behavior of conducting polypyrrole has not been extensively investigated in the FIR and microwave regime. In the present investigation, the dielectric constants and optical conductivities of conducting polypyrrole were determined at frequencies in the FIR by analysis of the reflection and transmission intensities at normal incidence. The measurements in the microwave region were carried out with a vector network analyzer. The behavior of the dielectric constants in FIR and microwave is discussed in the context of the Debye and the Drude models. The dependence of the dielectric constants of polypyrrole on doping in these frequency regions and the ability to manipulate these parameters during synthesis is demonstrated. The exploitation of this behavior will lead to new applications in the field of infrared optics and electronics in which precise control of such material characteristics as reflection, absorption, and conduction are critical.

II. SAMPLE PREPARATION

Conducting polymers such as polypyrrole may be simultaneously polymerized and doped at the working elec-

 0021-8979/91/020899-07$03.00

trode of an electrochemical cell. The use of appropriate electrolyte provides the dopant counterion. This approach leads to the growth of uniform thin films covering the entire working electrode. This is the method of choice when films with controlled thickness and tailored electrical properties are desired. The nature of dopant distribution and level of doping can be exactly controlled by controlling the current passed through the electrochemical cell. In addition, the film grows in intimate contact with the electrode and conforms to its shape. For dielectric measurements in the FIR and microwave regions, large area, smooth and flat films are essential.

Free-standing films of polypyrrole doped with tosylate anions were synthesized by using a platinum foil as the working electrode in an acetonitrile solution containing 0.1 M pyrrole and 0.25 M tetraethylammonium tosylate. A carbon plate serves as the counter electrode and a calomel reference electrode is used to monitor the working electrode potential during the galvanostatic synthetic process. By passing a current of 0.4 mA/cm^2 for a period of 4 h, oxidation and polymerization occur simultaneously, producing a black conducting film at the electrode. Films ranging in thickness from 5 to 50 μm were prepared. The film is immersed in acetonitrile for 15 min and dried under vacuum at room temperature.[8]

III. DATA ANALYSIS

Measurements of reflection (R) and transmission (T) intensities were performed in the far infrared (FIR) utilizing an FTIR (Fourier transform infrared) spectrometer. A Michelson interferometer modified to include an enlarged sample compartment has been used to carry out the measurements. Measurements of reflection and transmission were performed at normal incidence with an accuracy of 5%. As prepared, the polymer films were typically 5 cm $\times$ 5 cm square. The optical beam was apertured down to expose approximately 2 cm^2 of the sample. In the reflection measurement, the collimated output of the interferometer was collected, focused on the sample, and recollected in an approximate $f/5$ optics system consisting of two off-axis parabolic mirrors, a flat gold mirror and a TPX lens. The sample holder as well as the background mirror was mounted on a translation stage allowing for consecutive measurements of sample and background reflectance without breaking vacuum. In the transmission mode, the sample is mounted near the output aperture of the sample box and the radiation focused down to a spot size of approximately two centimeters.

A Mercury lamp source combined with mylar beam splitters of different thicknesses provides black body radiation in the spectral region between 10 and 100 cm^{-1}. The radiation power in the FIR is only a few nanowatts, and the transmittance of the polymer films may be less than 0.01 percent. A silicon bolometer cooled to 1.8 K with a sensitivity of 3×10^{-14} W/Hz$^{1/2}$ was employed for this reason. The entire system is operated under vacuum to reduce the signal loss associated with water absorption in the FIR.

To further enhance the reliability of the R and T data, additional measurements were performed with high-power (10 mW) HCOOH lasers at discrete frequencies for comparison with the FTIR data. The laser sources also extend data acquisition capability to frequencies below 8 cm^{-1}.

Determination of the real and imaginary parts of the complex index of refraction was accomplished by application of the Fresnel equations to measurements of R and T at normal incidence. The complex reflection (r) and transmission (t) amplitudes are given below:

$$r=\rho(1-e^{i\beta})/(1-\rho^2e^{i\beta}) \quad (1)$$

$$t=(1-\rho^2)e^{i\beta/2}/(1-\rho^2e^{i\beta}) \quad (2)$$

with $\rho=(1-n_c)(1+n_c)$ and $\beta=4\pi n_c d/\lambda$ where n_c is the complex index of refraction given by $n_c=n+ik$ and d is the film thickness.

Although it is frequently difficult to measure transmission in materials that are highly reflecting or absorbing, the use of sensitive detectors permits the direct determination of the complex index of refraction using the Fresnel equations. This is more convenient than the Kramers–Kronig method and especially useful when collecting data over a narrow frequency range. The Kramers–Kronig method depends on very accurate reflection measurements taken over a broad frequency range and extrapolation of data to estimate R_0 and R_∞.

The values of n and k obtained from the Fresnel equations are multiple valued functions of R and T. The transcendental nature of the equations requires a computerized numerical technique for their solution. We have developed software similar to that described by Nestell and Christy[9] in which one plots the constant contours of R and T in a plot of n vs k. The intersections of R and T give all the possible paired values of n and k satisfying the Fresnel equations and can be determined by a numerical root searching routine. As an example of this technique, in Fig. 1 the contours of constant reflection and transmission with $R=0.273$ and $T=0.125$ were plotted for a 55-μm-thick polypyrrole film (reduced 1/2 h) at 20 cm^{-1}.

The possible n and k roots satisfying the Fresnel equations for this polymer at 20 cm^{-1} are indicated in Table I. The selection of the physically correct root from among the

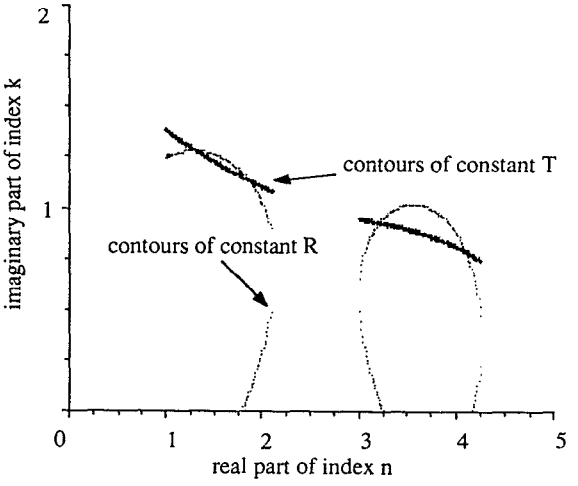

FIG. 1. Contours of constant R and T for a polypyrrole film (reduced 1/2 h) at 20 cm^{-1}.

TABLE I. Multiple root pairs for polypyrrole reduced 1/2 h measured at 20 cm $^{-1}$.

Real part of index n	Imaginary part of index k
4.10	0.78
3.21	0.92
1.85	1.13
1.32	1.28

possibilities indicated in Table I typically requires performing additional measurements.[9] A comparison of n and k derived from samples of different thicknesses will provide a common pair of physical roots. Another method employed in this study required performing an angle reflection scan using p-polarized radiation. The real part of the index of refraction was determined by locating the position of the reflection minimum at the Brewster angle.

Measurement of the complex permittivity was performed in the spectral region between 8.5 and 12.4 GHz using a HP8510 network analyzer. In this measurement the sample is held between two waveguides. The network analyzer measures the magnitude and phase of the signal transmitted and reflected by the sample. The signal from the source is separated into a component incident on the sample and a reference signal against which the magnitude and phase of the reflected and transmitted signals are compared. These signals are processed by the network analyzer to determine the complex reflection and transmission ratios. Calibration is performed using standards such as short and open circuits, a fixed load and a precise transmission line. The amplitude and phase angles are expressed as S parameters[10] from which such quantities as standing wave ratios (SWR), complex permittivity and permeability can be computed. Application of the appropriate boundary conditions allows one to find the complex reflection and transmission coefficients R and T. The reflection and transmission coefficients can be written as:

$$R = K \pm [K^2 - 1]^{1/2}, \tag{3}$$

where

$$K = \frac{S_{11}^2(\omega) - S_{21}^2(\omega) + 1}{2S_{11}(\omega)}. \tag{4}$$

The complex S parameters are defined as:

S_{11} = reflected amplitude/incident amplitude

and

S_{21} = transmitted amplitude/incident amplitude

$$T = \frac{[S_{11}^2(\omega) - S_{21}^2(\omega)] - R}{1 - \{S_{11}(\omega) + S_{21}(\omega)\}R}. \tag{5}$$

The complex permeability is then:

$$\mu_r = \frac{1 + R}{\Lambda(1 - R)\left(\frac{1}{\lambda_0^2} - \frac{1}{\lambda_c^2}\right)^{1/2}} \tag{6}$$

and

$$\frac{1}{\Lambda^2} = -\left[\frac{1}{2\pi d}\ln\left(\frac{1}{T}\right)\right]^2, \tag{7}$$

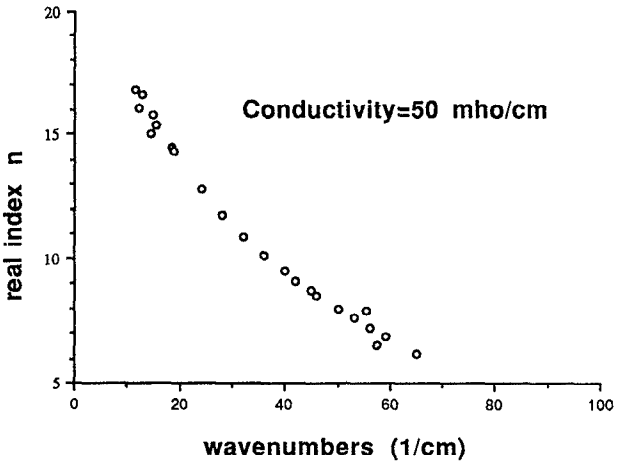

FIG. 2. Real part of the index of refraction for a heavily doped film Molar dopant ratio of tosylate anion to pyrrole = 0.35.

where d is the sample thickness, λ_0 = free space wavelength and λ_c is the cutoff wavelength of the waveguide. The complex permittivity is then given by:

$$\epsilon_r = \left[\frac{1}{\Lambda^2} + \frac{1}{\lambda_c^2}\right]\frac{\lambda_0^2}{\mu_r} \tag{8}$$

IV. RESULTS AND DISCUSSION

Figures 2 and 3 are plots of the complex index of refraction for fully oxidized films with measured dc conductivity of 50 Ω^{-1} cm^{-1}. The large dispersion of n and k is apparent in the doped (as grown) films. Reducing the polypyrrole films produces large variations in the measured levels of dc conductivity as well as the dielectric constants.

Figures 4 and 5 are plots of the complex index of refraction for films reduced 1/2 and 1 h, respectively. Typical conductivities for films of this type are 5.0 and 0.1 Ω^{-1} cm^{-1}, respectively.

The data indicate that the dielectric constants are highly

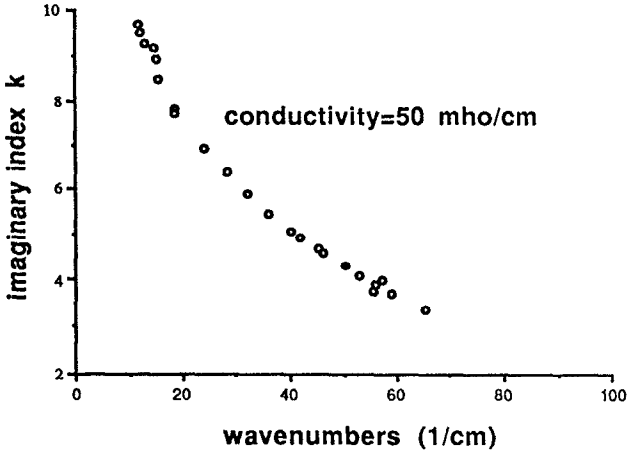

FIG. 3. Imaginary part of the index of refraction for a heavily doped film Molar dopant ratio of tosylate anion to pyrrole = 0.35.

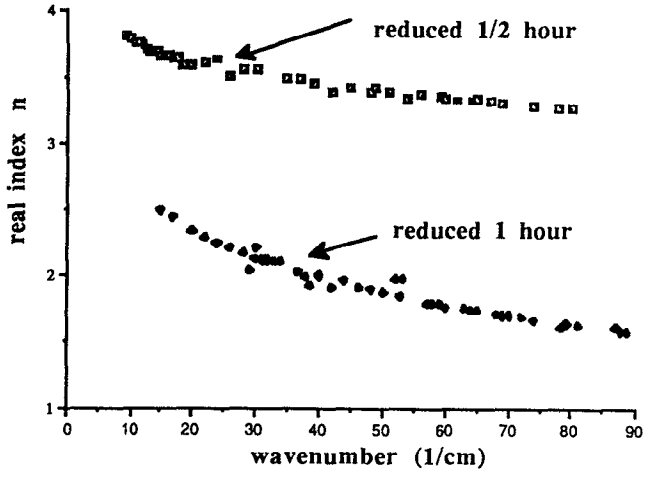

FIG. 4. Real part of the index of refraction for a reduced film reduction = 1/2 h (molar dopant ratio of tosylate anion to pyrrole = 0.28) and 1.0 h.

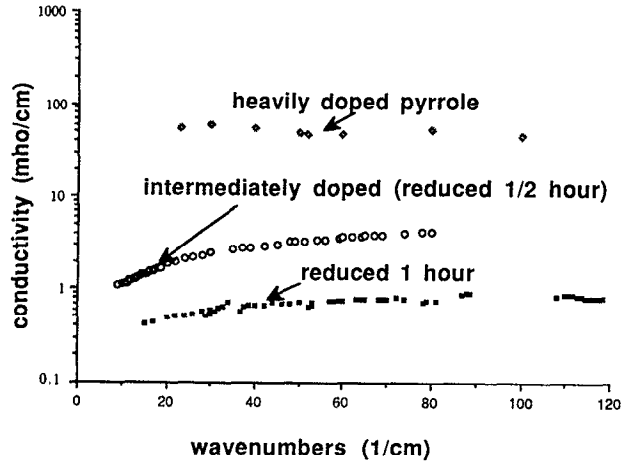

FIG. 6. Conductivity of polypyrrole as a function of doping level.

dispersive in the heavily doped films. The values of n and k can be varied over a broad range by controlling the level of doping. In Fig. 6 the optical conductivity is plotted as a function of doping for films ranging between heavily doped and reduced 1 h in which the conductivity of polypyrrole is seen to vary over three orders of magnitude.

The dielectric measurements made on doped polypyrrole in the FIR were compared to measurements made at microwave frequencies between 0.1 and 1 cm^{-1}. Significantly larger values of n and k were measured at these frequencies. The complex index of refraction is plotted as a function of frequency (8.5–12.5 GHz) in Fig. 7. Additional measurements in the microwave will be produced in a later publication.

The average values of n and k of the films studied at 10 cm^{-1} are described in Figs. 8 and 9. The real and imaginary parts of the complex index of refraction are given as a function of reduction time. The results demonstrate the very large variation in dielectric behavior achieved through the oxidation-reduction process. The dielectric properties of polypyrrole as determined in this investigation are compared to measurements reported by other researchers.[3,7,11–13] These results are presented in Table II.

The frequency dependence of the complex dielectric constants and the optical conductivity are inconsistent with the predictions given by a simple metal theory, such as the Drude free-carrier model. The dielectric functions, as given by the Drude model, take on different limiting forms depending upon the relationship between the frequency ω and the dielectric relaxation time.

The conductivity of the heavily doped film of Fig. 6,

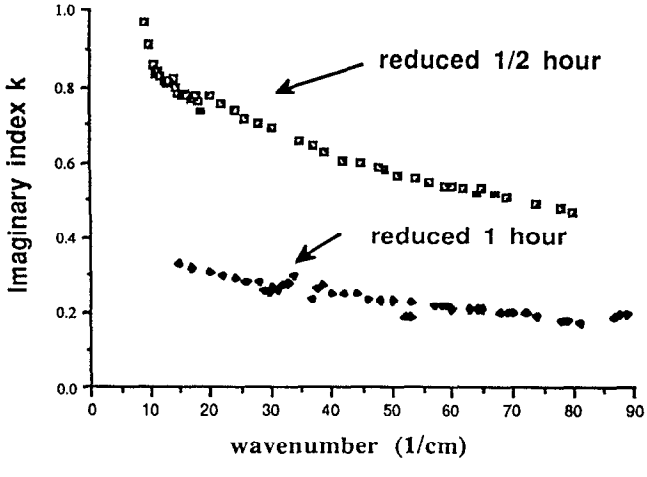

FIG. 5. Imaginary part of the index of refraction for a reduced film reduction = 1/2 h (molar dopant ratio of tosylate anion to pyrrole = 0.28) and 1.0 h.

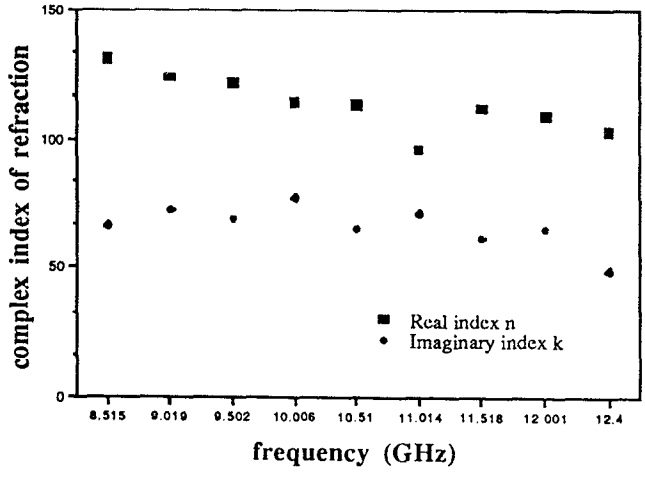

FIG. 7. n and k at microwave frequencies for a polypyrrole film dopant ratio of tosylate anion to pyrrole = 0.35.

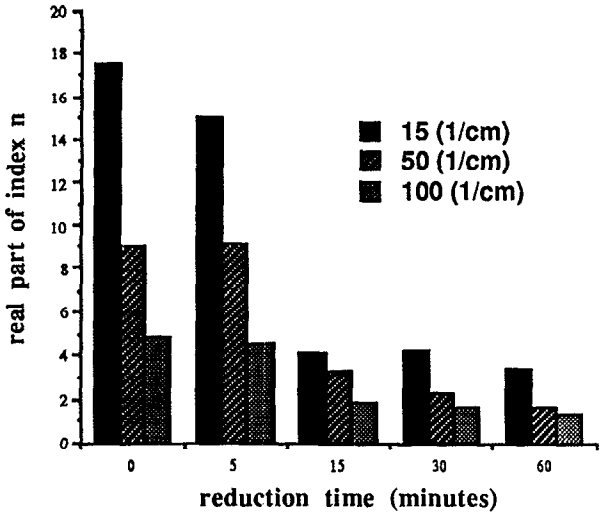

FIG. 8. Real part of the index of refraction as a function of doping.

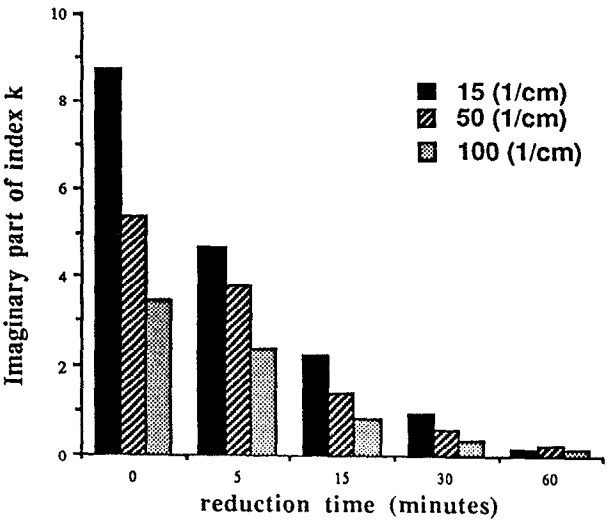

FIG. 9. Imaginary part of the index of refraction as a function of doping.

given by $\sigma_{opt} = \omega\epsilon_2 = 2\omega nk$, is slowly varying in the 10–100 cm^{-1} region. The large and dispersive nature of the dielectric constants in the FIR is evident from the data plotted in Fig. 10. The complex dielectric constants plotted in Fig. 10 display a monotonically decreasing frequency dependence. For the case $\omega\tau \gg 1$, the Drude model fails to account for the observed dc conductivity. For the alternative case $\omega\tau \ll 1$, it is readily shown that the real part of the dielectric constant ϵ_1 does not display the constant behavior necessary to fit the Drude model.

Zuo[13] *et al.* successfully fit dielectric data determined at low frequencies ($10^1 - 10^6$ Hz) for conducting emeraldine polymer ($\sigma = 5\ \Omega^{-1}\ cm^{-1}$). It was concluded that the dielectric response was the sum of two terms, one associated with the polymer backbone plus a contribution due to the hopping of charge carriers between singly and doubly charged defect states. From the Debye model, the relaxation time was estimated to be on the order of 10^{-10} s.

The dielectric data obtained from doped polypyrrole films are discussed in the context of the Debye relaxation model. The Debye representations of the complex dielectric constants are easily shown to be given by:[14]

TABLE II. Dielectric properties of several polymers and copper.

Study	Polymer	dc cond. mho/cm	Frequency cm^{-1}	n	k	ϵ_1	ϵ_2	opt. cond. mho/cm	$\alpha(cm^{-1})$
Hasagawa[a]	A	32	10.0–90	10.9–6.5	8.9–1.9	39.3–38.7	192–25	32–38	1120
Hasagawa[b]	B	320	10.0–90	32–15	31–13	62.7	1940–390	323–325	3900
Phillips et al.[c]	C	50	20–200	16.4–4.1	4.6–2.0	250–13	150–16	50–54	1160
Phillips et al.[c]	C	50	13–56	20–3.7	6.5–4.0	360–(−2)	262–30	58–27	1060
Phillips et al.[c]	C	90–100	18–41	17.5–11.6	7.1–5.7	255–101	250–131	84–101	1600
Phillips et al.[c]	C	65	20	18.5	5.3	314	196	65	1330
Phillips et al.[c]	C	50	0.28	130	66	12712	17374	81	232
IBM[d]	B	x	200	3	1.8	6	12	40	4500
Ordal[e]	D	10^6	180	61	313	-9×10^4	3.8×10^4	1×10^6	7×10^6

[a] see Ref. 11
[b] see Ref. 2
[c] this study
[d] see Ref. 6
[e] see Ref. 10
A = P3MT
B = polypyrrole perchlorate
C-polypyrrole tosylate
D = copper

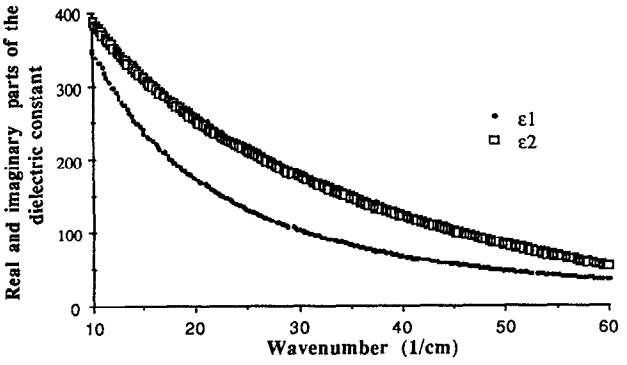

FIG. 10. Real and imaginary parts of the complex dielectric constants for a doped polymer in the FIR. Molar dopant ratio of tosylate anion to pyrrole = 0.35.

$$\epsilon = \epsilon_\infty + \frac{(\epsilon_0 - \epsilon_\infty)\omega_\tau}{(\omega_\tau + i\omega)}, \tag{9}$$

$$\epsilon_1 = \epsilon_\infty + \frac{(\epsilon_0 - \epsilon_\infty)\omega_\tau^2}{(\omega^2 + \omega_\tau^2)}, \tag{10}$$

$$\epsilon_2 = \frac{(\epsilon_0 - \epsilon_\infty)\omega\omega_\tau}{(\omega^2 + \omega_\tau^2)}, \tag{11}$$

where

$$\omega_\tau = \tau^{-1}. \tag{12}$$

The values of dielectric constants were determined to be on the order of 10^4 in the microwave, (Fig. 11) and $10^1 - 10^2$ in the FIR regimes (Fig. 10). In addition, both the real and imaginary parts of the complex dielectric constant were found to be monotonically decreasing functions of frequency. The Debye model can be made qualitatively consistent with the measurements of this study if one assumes a dielectric relaxation time on the order of 10^{-10} s. Under these conditions, the model equations, (10) and (11), provide for a nearly constant optical conductivity (within an order of magnitude change over the frequency range) and for $\epsilon_2 > \epsilon_1$, as observed in the data.

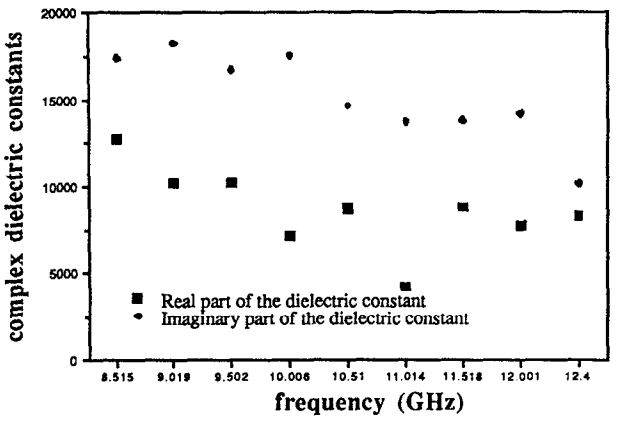

FIG. 11. Real and imaginary parts of the complex dielectric constants for a doped polymer in the microwave; Molar dopant ratio of tosylate anion to pyrrole = 0.35.

Both the FIR and microwave measurements were made over narrow frequency ranges when compared to the very broad absorption peak in ϵ_2. Additional data are required over a broader frequency range to attempt a quantitative fit. However, qualitatively, measurements made in both the FIR and microwave are consistent with the Debye model. Further measurements in the microwave at lower frequencies will be undertaken to determine more precisely the nature of the dielectric relaxation mechanism.

V. CONCLUSIONS

In this study, the constant behavior of ϵ_1 necessary for polypyrrole to exhibit simple metal like conductivity under the Drude assumptions is not observed. The Debye model allows for the observed dispersion in both ϵ_1 and ϵ_2. A slow dielectric relaxation time, τ, on the order of $10^{-9} - 10^{-10}$ s, is reasonable in the context of our measurements and also consistent with the work of Zuo[13] *et al.* for another class of conducting polymers.

The heavily doped films exhibit large real and imaginary parts of the complex index of refraction $(n + ik)$ and are highly dispersive in the FIR frequency region. The magnitude of these quantities is changed significantly when the conductivity is decreased through the process of reduction. The relationship between the reduction time and the resultant dielectric behavior is described in Figs. 8 and 9. The ability to tailor the dielectric properties of conducting polymer films in the FIR and microwave regime is one of the significant outcomes of this research. The exploitation of these capabilities may lead to new applications in the field of infrared optics and electronics in which precise control over such material characteristics as reflection, absorption, and conduction are critical.

The dielectric behavior of these materials suggests applications at lower frequencies and measurements are being extended to the microwave region where the complex index of refraction is observed to be large and slowly varying (Fig. 7). Under these circumstances, the materials continue to be highly reflective as in the FIR, but have smaller absorption coefficients and exhibit less loss. For example, between 0.33 and 20 cm^{-1}, α varies from 200 to 3000 cm^{-1}, and the skin depth changes from $\delta_{(1/e)} = 40$ to $3\,\mu$ (doped polypyrrole). These material properties in the microwave are useful in the fabrication of devices such as Fabret-Perot etalons. Such measurements are presently being performed in the 8–40 GHz range using the HP 8510A network analyzer. Polypyrrole films of different conductivities and thicknesses are candidate materials for developing a microwave bandpass filter. The requirements for such a device include a large index of refraction at microwave wavelengths and suitably low loss.

[1]H. Shirakawa, E. J. Louis, A. G. MacDiarmid, C. K. Chiang, and A. J. Heeger, J. Chem. Commun **1977**, 578 (1977).
[2]C. D. Peres, J. M. Pernaut, and M. A. De Paoli, Synthetic Metals **28**, C57 (1989).
[3]S. Hasagawa, K. Kamiya, and J. Tanaka, Synthetic Metals **14**, 97 (1986).
[4]K. Kanazawa, A. F. Diaz, W. D. Gill, P. M. Grant, G. B. Street, Synthetic Metals **1**, 329 (1979/1980).
[5]G. B. Street, T. C. Clarke, W. Volksen, and J. Economy, IBM J. Res. Devel. **27**, 321 (1983).

[6]J. C. Scott, P. Pfluger, M. T. Krounbi, and G. B. Street, Phys. Rev. B **28**, 2140 (1983).
[7]K. Yakushi, L. J. Lauchlan, T. C. Clarke, and G. B. Street, J. Chem. Phys. **79**, 4774 (1983).
[8]L. J. Buckley, D. K. Roylance, and G. E. Wnek, J. Polym-Sci: Part B **25**, 2179 (1987).
[9]J. E. Nestell, Jr. and R. W. Christy, Appl. Opt. **3**, 643 (1972).
[10]A. M. Nicolson, G. F. Ross, IEEE Trans. Instrum. Meas. **IM-19**, 377 (1970).
[11]M. A. Ordall, R. J. Bell, R. W. Alexander, Jr., L. L. Long, and M. R. Querry, Appl. Opt. **24**, 4493 (1985).
[12]S. Hasagawa, K. Kamiya, and J. Tanaka, Synthetic Metals, **18**, 225 (1987).
[13]F. Zuo, M. Angelopoulos, and A. G. MacDiarmid, A. J. Epstein, Phys. Rev B **6**, 39 (1989).
[14]N. E. Hill, *Dielectric Properties and Molecular Behavior* (Van Nostrum Reinhold, London, 1969).